

《Original》

## Calculation of Nuclear Characteristics of the TRIGA Mark-III Reactor

Chong Chul Yook\* and Gee Yang Han

Han Yang University

Byung Jin Jun, Ji Bok Lee and Chang Kun Lee

Korea Advanced Energy Research Institute

(Received October 21, 1981)

## TRIGA Mark-Ⅲ 원자로의 노심특성계산

육 종 철 · 한 기 양

한양대학교

전병진 · 이지복 · 이창건

한국에너지연구소

(1981 10. 21 접수)

### Abstract

A simulation procedure which can represent time-dependent nuclear characteristics of TRIGA Mark-III reactor is developed. CITATION, a multi-group diffusion-depletion program, has been utilized as calculational tool. The group structure employed in this study consists of 7 groups: -3-fast and 4-thermal-which is conventionally utilized in TRIGA type reactor analysis.

Three-dimensional nuclear characteristics are synthesized by combining results from two-dimensional plane calculation and two-dimensional cylinder calculation, since direct three-dimensional approach is not yet possible. An effort is made to develop a method which can extract effective zone and group dependent bucklings by neutron diffusion theory rather than conventional zone and/or group independent bucklings by neutron transport theory, since neutron leakage is quite high for small core such as research reactors. It is turned out that the method developed in this study gives satisfactory results.

The calculation is performed under assumptions that all control rods are fully withdrawn, that no samples are inserted in the irradiation holes and that the core is located in the center of the reactor pool.

Burnup-dependent variation of core excess reactivity, time dependent change of Xe-135 poisoning and reactivity worth of rotary specimen rack are calculated and compared with operation records. Neutron flux and power distribution as well as neutron spectrum in each irradiation facility are presented.

\*Admission Committee, International Radiation Protection Association (IRPA)

## 요 약

TRIGA Mark-III 원자로의 핵특성을 실제 운전상태와 유사하게 모사할 수 있는 해석절차를 개발하였다. 계산에 사용한 전산코드는 다중중성자확산 연소계산코드인 CITATION이고 채택한 중성자 에너지군의 수는 TRIGA형 원자로에서 일반적으로 사용하는 7군(고속영역 3, 열영역 4)이다.

직접적인 3차원 계산이 현실적으로 불가능하므로 평면 2차원계산과 원통형 2차원 계산으로 3차원 효과를 기하였다. 연구로와 같이 노심이 작은 원자로에 대하여는 중성자평형에서 buckling에 의한 효과가 매우 크기 때문에 이를 정확하게 나타내는 방법의 개발에 중점을 두었다. 본 연구에서는 에너지군 또는 영역에 무관한 buckling을 중성자 수송이론으로 산출하는 전형적인 방법을 사용하지 않고 중성자 확산이론으로서 에너지군별, 영역별 buckling을 산출하였으며, 이를 이용하여 수행한 노심계산의 결과는 만족스러웠다. 계산시 노심은 원자로수조의 중앙부에 있는 것으로 하고 제어봉은 완전히 인출되었으며 동위원생산용 조사시료는 없는 것으로 가정하였다.

계산결과로서 연소에 따른 초과반응도가의 변화, 운전이력에 따른 Xe-135 독작용의 변화, 회전 조사시료대의 반응도가를 산출하고 이를 실제 운전자료와 비교하였다. 또한 중성자속 및 출력분포, 노심 각 조사시설에서의 중성자 스펙트럼등에 대한 계산결과도 제시하였다.

### I. Introduction

In recent years, demand for the utilization of TRIGA Mark-III reactor has shown to be remarkable especially in the areas of radioisotope production and reactor material testing. To meet such ever-increasing demand, it was indispensable to install more irradiation holes in inner region of the core, which eventually requires generating accurate nuclear characteristic data.

This paper is intended to describe the method of calculational procedure adopted herein for the clarification of in-core nuclear characteristics of Korean TRIGA Mark-III reactor and its aftermath with the comparative data resulted from the actual operational logbook.

The calculational approach for the intended task has, however, been faced with difficult barriers due to complicated operational history and ever-replacing irradiation specimens in the reactor core. Since this reactor cannot attain an equilibrium core state, despite nearly its 10-year operation history, some sort of core simulation covering the entire operational period from its

criticality in April 1972 to date was inevitable to take place in an attempt to grasp the current nuclear characteristics by and large. Fortunately, this core was loaded with fresh FLIP (Fuel Lifetime Improvement Program) fuel elements except for 6 irradiated standard fuels (20% enriched, 8.5% uranium loaded) positioned in B-ring in 1979.<sup>1,2)</sup>

The number of irradiated standard fuels was then merely 6 out of the total 97, and the burnup rate of U-235 depleted thus far in these 6 fuels was reckoned up to be less than 13%. Referring to their previous irradiation history, an approximate estimation of isotope concentration in these fuels could be made at nearly negligible deviation, should the said point of time be adopted as the beginning of core life. This core configuration remained unchanged up until January 1981.

This paper explains how the preliminary study of establishing simulation model of TRIGA Mark-III reactor with its operation history was carried out, as to how the applicability of this model by comparing the results with experimental data and operational record from April 1978 to

December 1980 was measured, and, at the same time, how the isotopic concentrations was generated for the further simulation of this reactor.

For this end, a multi-group diffusion depletion code, entitled "CITATION",<sup>3)</sup> and 7-neutron energy group constants made available to us by the courtesy of Messrs<sup>4)</sup>. General Atomic Company were used so as to figure out 2-dimensional hexagonal core flux and power distribution. Zone- and group-dependent axial Bucklings as well as axial heterogeneous effects of rotary specimen rack, etc., were calculated by means of 2-dimensional cylindrical approach. For simplicity and also convenience' sake, irradiation samples for radioisotope production and activation analysis together with control rods were exempted from our consideration in calculation.

The variation of Xe-135 poisoning effects attributed to unsteady state operational mode and the neutron spectra in incore irradiation facilities have, also, gone through evaluation from the resulted data of the above core calculation.

## II. Calculational Procedure

### II.1. TRIGA Mark-III Core Characteristics

This reactor is swimming pool type and is cooled by natural convection of light water in the pool. The core is translocated from one place to another according to the utilization purpose such as radioisotope production, experiments of neutron physics at beamports or use of exposure room. When the core is positioned at the center of pool, radioisotope production becomes the main purpose of reactor operation, and, for this end, the outcore irradiation facility,

namely, rotary specimen rack or simply Lazy Susan, is lowered downward around the active core so as to get the maximum neutron flux. If the core is moved to the end of the pool so that the core is positioned either next to the neutron beamports or the exposure room, rotary specimen rack must be raised upward for more neutron effluence toward the beamports or exposure room. There are 41 sample receptacles in the rotary specimen rack, and the main structural material consists of aluminium;<sup>5)</sup> however, other space in the rack is filled in with air.

121 fueling holes arranged in hexagonal geometry are supported by upper and bottom aluminium grids, and these grids are supported by cylindrical aluminium shroud. The rotary specimen rack is located around the shroud when it is downed.

Each fueling position can be loaded either with fuel rod, control rod, fission chamber, pneumatic tube or irradiation hole. Figure 1 shows the core arrangement composed in April 1979. There are 97 fuel elements consisting of 6 standards and 91 FLIP's including 4 fuel-follower control rods, one transient control rod, 3 fission chambers, one pneumatic tube, one central thimble, 2 irradiation holes and 16 water holes. Figure 2 illustrates axial view of these rods.

Fuel rod is composed of solid zirconium rod at center, U-ZrH<sub>1.6</sub> as fuel and moderator clad with SS-304 cladding material.<sup>6)</sup> Axial portion of fuel at both sides is filled in with carbon as reflector. Uranium quantity in fuel zone is 8.5% of the alloy, whereas U-235 enrichment is 20% for standard and 70% for FLIP, respectively.

Axial view of the core is depicted in Figure 3.

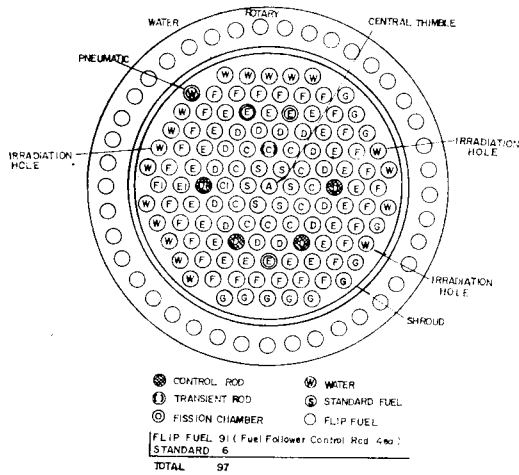


Fig. 1. Core Diagram Arranged in April 1979

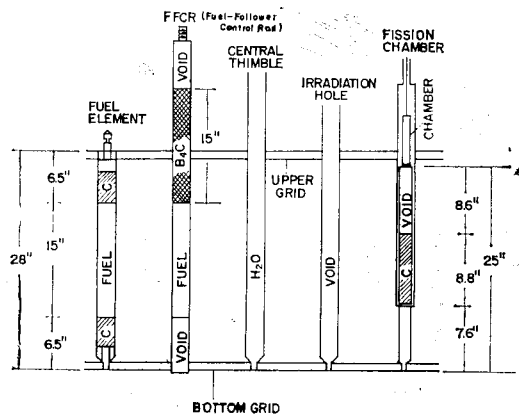


Fig. 2. Axial Views of Rods

II. 2. Geometric Modeling for Core Calculation

The arrangement of rods in the core is hexagonal, but shroud and rotary specimen rack have cylindrical geometry. For simplicity, hexagonal geometry is adopted for radial 2-dimensional calculation, and the region of shroud and rotary specimen rack is modified for this calculation. Figure 4 is the geometric model for hexagonal calculation, adopted by the view so that as much real shape and volume can be reflected as

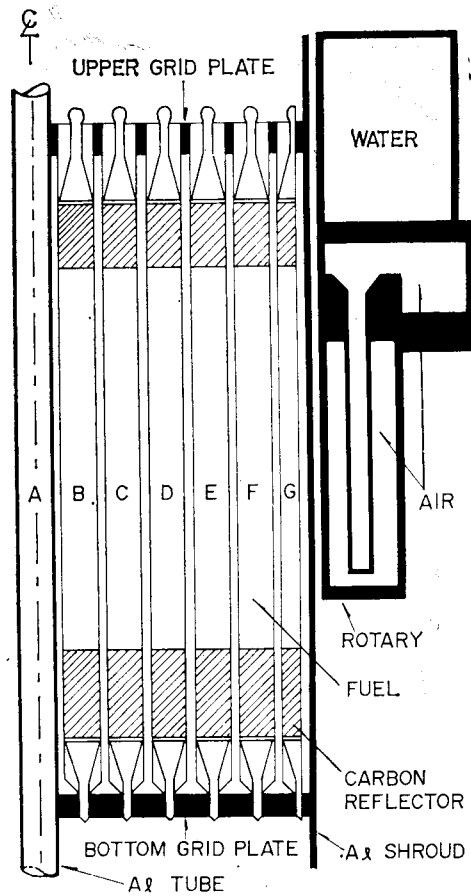


Fig. 3. Axial Views of Core

possible.

On the contrary, each ring should be modified from hexagonal to cylindrical geometry for cylindrical 2-dimensional calculation.<sup>7)</sup> This job is tedious but relatively easy because hexagonal shape is convenient for conversion into cylindrical. Figure 5 shows cylindrical model adopted in this work. In the upper and bottom grid zones, grid plates and end fittings of fuel rods are included taking their material composition into account.

II. 3. Core Calculation

To represent core characteristics by 2-

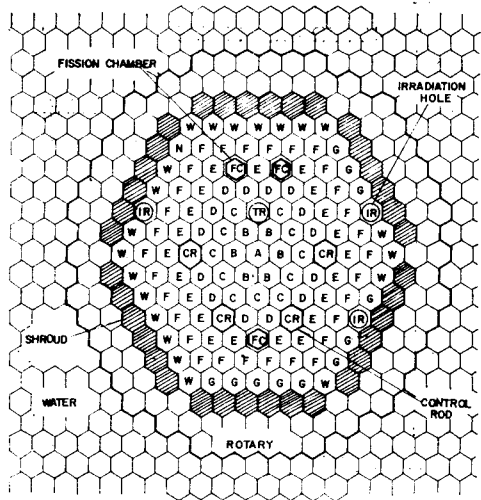


Fig. 4. Hexagonal Geometry for 2-Dimensional Calculation of TRIGA Mark-III Reactor Core

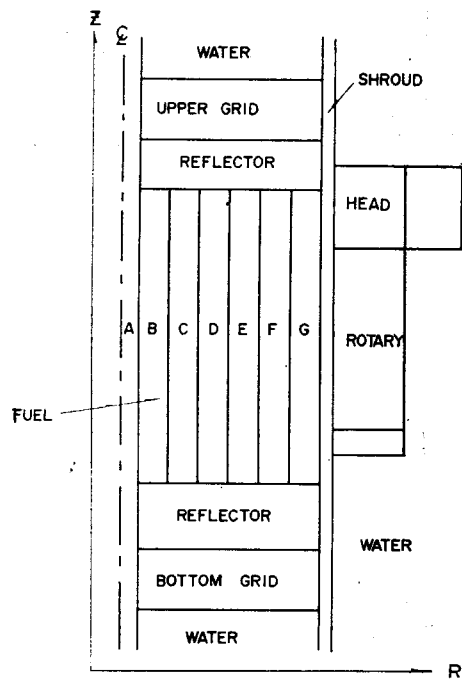


Fig. 5. R-Z Cylindrical Calculation Model

dimensional calculation, the effect of another dimension exempted from consideration should be represented accurately by all means. For 2-dimensional hexagonal calcu-

lation, the determination of axial Bucklings ( $B_z^2$ ) and axial homogenizations for heterogeneous regions are main task to be carried out in advance, while, for 2-dimensional cylindrical calculation, ring homogenization is the main objective. But these works cannot be performed by exclusive calculation. In other words,  $B_z^2$  and axial homogenization effects should be obtained from the result of R-Z cylindrical calculation, and, at the same time, ring homogenization can be accomplished by radial 2-dimensional calculation. Figure 6 represents the procedure used in this study which was employed to get the above problem settled down. In general, neutron transport theory is applied to the acquisition of  $B_z^2$  as neutron leakage term at the core axial boundaries. In this study, however, it is obtained from cylindrical diffusion calculation based on the following method. Multi-group neutron diffusion equation<sup>8)</sup> is represented as,

$$-D_g \nabla^2 \phi_g + \sum_{R_g} \phi_g = \text{Source}_g + \text{Sin}_g \dots (1)$$

- where  $g$  = neutron energy group
- $D$  = diffusion coefficient
- $\phi$  = neutron flux
- $\sum_R$  = removal cross-section
- Source = neutrons generated from fission
- Sin = neutrons scattered in from other groups.

In Eq. (1), the Laplace operator  $\nabla^2$  can be separated by radial and axial terms. And then Eq. (1) can be integrated for certain zone, such as,

$$-D_g \nabla^2 \phi_g V - 2A D_g \frac{\partial \phi_g}{\partial Z} + \sum_{R_g} \phi_g V = (\text{Source}_g + \text{Sin}_g) V \dots (2)$$

where  $V$  = volume of the zone

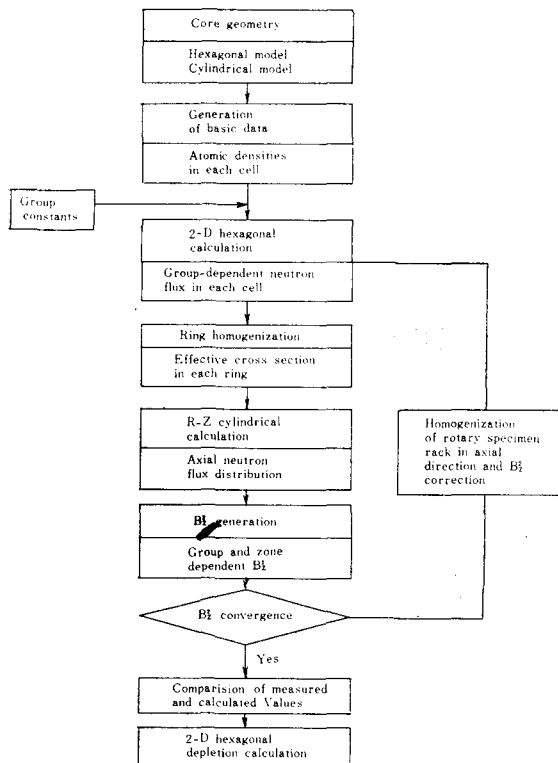


Fig. 6. Calculation Procedure

A=upper or bottom surface area  
 $\phi_s$ =neutron flux at upper or bottom surface area.

If we divide Eq. (2) by volume  $V(=AH)$ ,

$$-D_g \nabla^2 \phi_g - \frac{2}{H} D_g \frac{\partial \phi_{sg}}{\partial Z} + \sum R_g \phi_g = \text{Source}_g + \text{Sin}_g \dots (3)$$

The second term in Eq. (3) represents the axial neutron leakage, and it is equal to  $B^2_{zg} \overline{D_g \phi_g}$ .

So  $B^2_{zg}$  can be extracted as,

$$B^2_{zg} = -\frac{2}{H} \frac{\partial \overline{\phi_{sg}}}{\partial Z} \dots (4)$$

In this study, group- and zone-dependent Bucklings obtained by Eq. (4) are used, and it is verified that they represent axial leakage to considerable accuracy.

Axial and ring homogenizations are to

modify neutron cross-sections so as to adjust neutron reaction rate for the zone composed of different cells. That is;

$$\overline{\phi} \overline{\sigma} \overline{N} V = \sum_i \phi_i \sigma_i N_i V_i \dots (5)$$

where  $\overline{\phi}$ =average neutron flux of the zone  
 $\overline{\sigma}$ =homogenized cross-section of the zone

$\overline{N}$ =homogenized atomic density

$V$ =total volume of the zone

$i$ =represents each cell.

#### II. 4. Xenon Poisoning with Operating History

TRIGA Mark-III reactor has been put in operation routinely on weekly basis except Sunday and Monday for weekly check. So the amount of Xenon usually doesn't reach up to equilibrium, yet it varies from time to time. The atomic density of Xe-135 at power can be represented as follows for certain zone:<sup>9)</sup>

$$N = \frac{Y_{Xe} + Y_I}{\lambda_{Xe} + \phi \sigma_{Xe}} [1 - e^{-(\lambda_{Xe} + \phi \sigma_{Xe})t}] - \frac{Y_I - I_0 \lambda_I}{\lambda_{Xe} + \phi \sigma_{Xe} - \lambda_I} [e^{-\lambda_I t} - e^{-(\lambda_{Xe} + \phi \sigma_{Xe})t}] + N_0 e^{-(\lambda_{Xe} + \phi \sigma_{Xe})t} \dots (6)$$

where  $Y_{Xe}, Y_I$ =generation rate of Xe-135 and I-135 from fission  
 $\lambda_{Xe}, \lambda_I$ =decay constant of Xe-135 and I-135

$\sigma_{Xe}$ =capture cross-section of Xe-135 (spectrum weighted)

$\phi$ =total neutron flux

$N_0, I_0$ =initial atomic density of Xe-135 and I-135.

Xenon poisoning is proportional to its capture rate and can be represented as;

$$\rho_{xe} = A \sum_i \phi_i V_i \sigma^i_{Xe} N_i \dots (7)$$

where  $i$ =each zone of the core

$V$ =zone volume

$A$ =normalization factor,

if variation of flux with Xe-135

atomic density is neglected.

The normalization factor A can be extracted from core calculations at the condition of no xenon and equilibrium xenon.

### II. 5. Estimation of Thermal Neutron Spectra in Irradiation Facilities

For well thermalized reactor, the thermal neutron spectrum can be represented by the combination of Maxwellian and 1/E distribution,<sup>10)</sup> such as

$$\phi(E) = \phi_M(E, T_n) + \lambda \frac{(E/kT_n)}{E} \dots\dots\dots (8)$$

where  $\phi_M$  = Maxwellian neutron flux

$T_n$  = effective neutron temperature

$\lambda$  = normalization factor

$\Delta(E/kT_n)$  = joining function

$k$  = Boltzmann constant.

The joining function has similar shape to unit step function. It begins to have value near  $E=4kT_n$  and has unit value after  $7\sim 8kT_n$ . There remain two unknowns,  $T_n$  and  $\lambda$ , if  $\Delta$  is approximated as unit step function.

7 group energy structure is shown in Table 1. The upper energy of group 6 is near  $5kT_n$ , while that of group 5 is near Cd cut-off energy region. So,  $T_n$  and  $\lambda$  can be extracted from 5, 6 and 7 group fluxes with such assumption that joining function has unit value above 0.14eV.<sup>11,12)</sup>

Table 1. Structure of Neutron Energy Groups

Energy Group	No.	Energy Region
Fast	1	15MeV~0.608MeV
	2	608KeV~9.12 KeV
	3	9.12KeV~1.125 eV
Thermal	4	1.125 eV~0.42 eV
	5	0.42 eV~0.14 eV
	6	0.14 eV~0.05 eV
	7	0.05 eV~0.002 eV

## II. Results and Discussion

Calculated effective multiplication factors

and Xe-135 poisoning variation are compared with experimental data and operation record. On the basis of these calculated figures, core flux distribution and thermal neutron spectra in irradiation facilities which have never been measured up until now have resulted from our continuous calculation work.

### III. 1. Core Effective Multiplication Factors

Calculated effective multiplication factors ( $k_{eff}$ ) for the initial core conditions have good agreement with experimental results. Two-dimensional hexagonal depletion calculation can, therefore, be carried out with much confidence such that calculation model is pertinent to a great degree.

The effective multiplication factors of the initial core are given in Table 2. It is assumed in the depletion calculation that the reactor is operated at the pool center with rotary specimen rack positioned adjacent to the active core.

Hexagonal calculation without rotary specimen rack is, therefore, not performed in this study. Variation of  $k_{eff}$  with operating history is illustrated in Figure 7. Data with equilibrium xenon cannot be extracted from operation logbook because this reactor had never reached any xenon equilibrium. On Tuesday, remaining xenon in the core can be neglected because of long decay time during weekend which is also followed by Monday shutdown for weekly check.  $k_{eff}$  points with no xenon condition are obtained from operation data on Tuesday. Only on 2 MW datum point is presented because this reactor has not been operated at 2MW full power since April 1979.

Weekly  $k_{eff}$  variation due to xenon poisoning is compared in the following section.

**Table 2. Initial Core Multiplication Factors (2MW, All rods out, No xenon)**

	Measured Value	Calculated Value			
		Cylindrical	Difference (%)	Hexagonal	Difference (%)
With Rotary Specimen Rack	1.01651	1.01489	0.16	1.01605	0.045
Without Rotary Specimen Rack	1.02328	1.02197	0.13	—	—
Reactivity Worth of Rotary Specimen Rack (Dollars)	-0.93	-0.975	4.9	—	—

**III. 2. Variation of Xenon Poisoning with Operation**

Xenon poisoning is the dominant factor in reactivity which is subject to vary during weektime operation. Poisoning effect resulted from Sm-149 and other fission products varies very slowly, and therefore can be neglected in terms of reactivity change versus time. The amount of reactivity variation due to coolant and fuel temperature variation can, also be neglected. Therefore, it is taken for granted that weektime variation of excess reactivity in the core is solely attributed to xenon poisoning variation.

activity variation falls in relatively good agreement with the operating history, although some points show somewhat large differences in between. Taking account of unavoidable errors in reading control rod positions and their reactivity worth curves as large as several tenths of an hour variation in core reactivity, it is then easily asserted that the calculational estimate of xenon poisoning does show quite accurate value as a whole.

**III. 3. Neutron Flux Distribution**

Measurement of in-core flux distribution with satisfactory accuracy is extremely hard in case of this reactor since sensor installation is extremely difficult and flux shape is very sharp. Therefore, calculational approach turns out to be the most convenient and less expensive means since it enables to simulate this core if its accuracy is verified.

Accuracy of this study is verified in core  $k_{eff}$ , rotary specimen rack effect and xenon effect. Unfortunately, however, measured data comparable in flux distribution are not readily available. Consequently only calculated flux distribution is presented in this paper leaving its verification as the future settlement.

Radial flux distribution is illustrated in Figure 10. Flux shape for hexagonal geometry is obtained by sweeping the line from F-6 to F-21. Differences in shapes

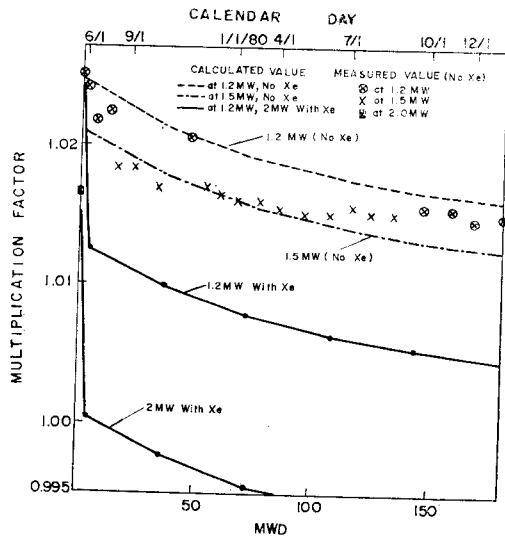


**Fig. 7.  $k_{eff}$  Variation with Burnup**

Comparison is made in Figures 8 and 9 between the calculated results and the actual operational data. The trend of rea-



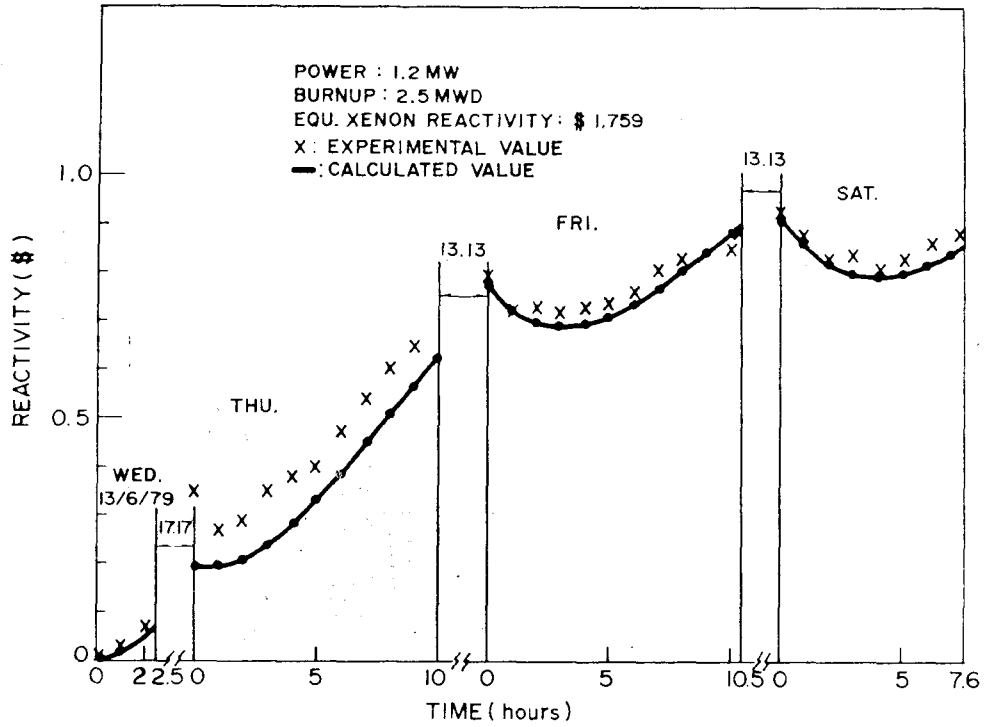


Fig. 8. Variation of Xenon Poison with Reactor Operation (I)

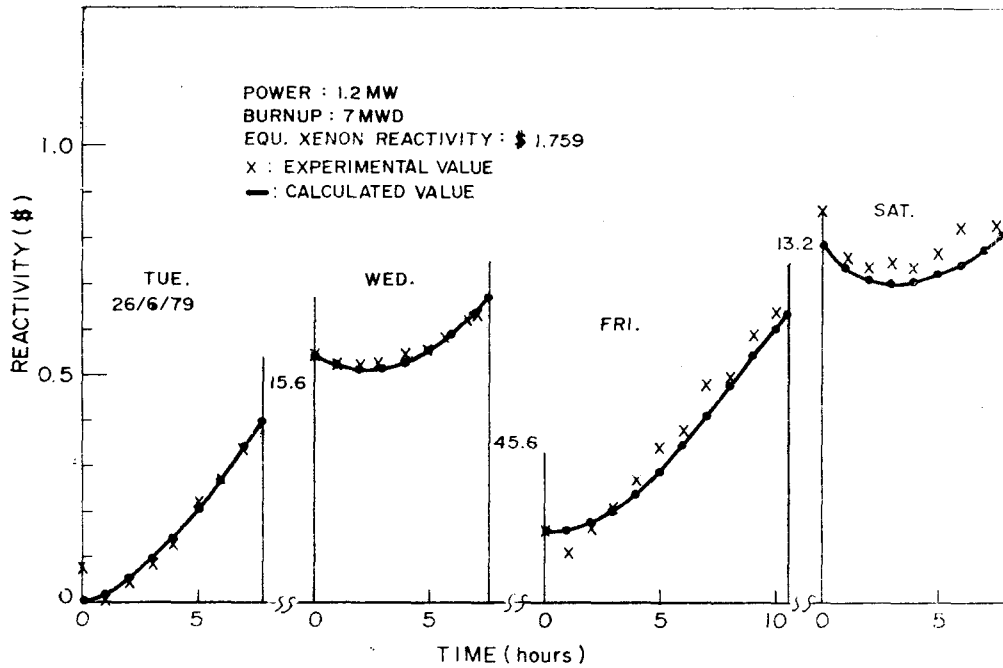


Fig. 9. Variation of Xenon Poison with Reactor Operation (II)

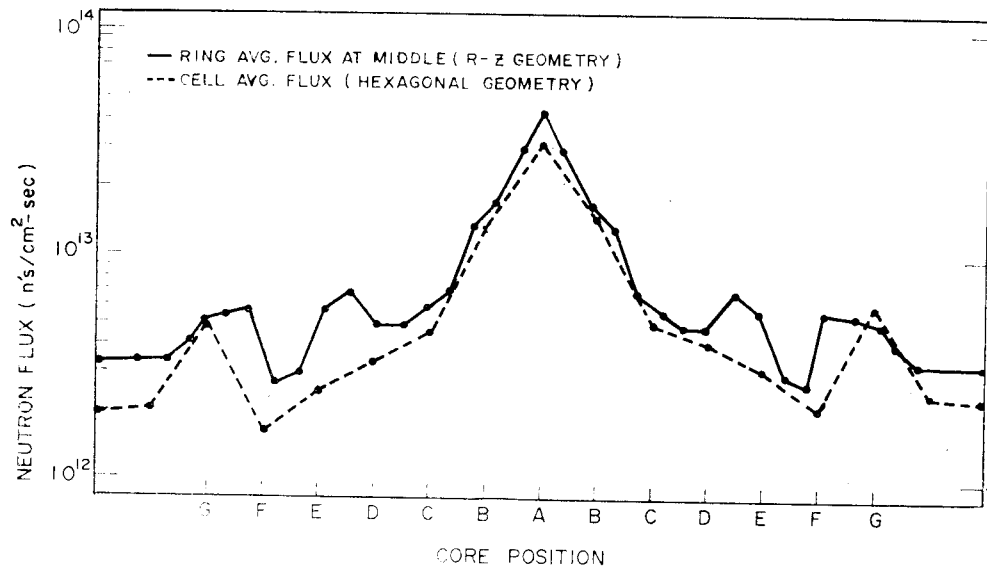


Fig. 10. Neutron Flux Distribution in Radial Direction at 1MW

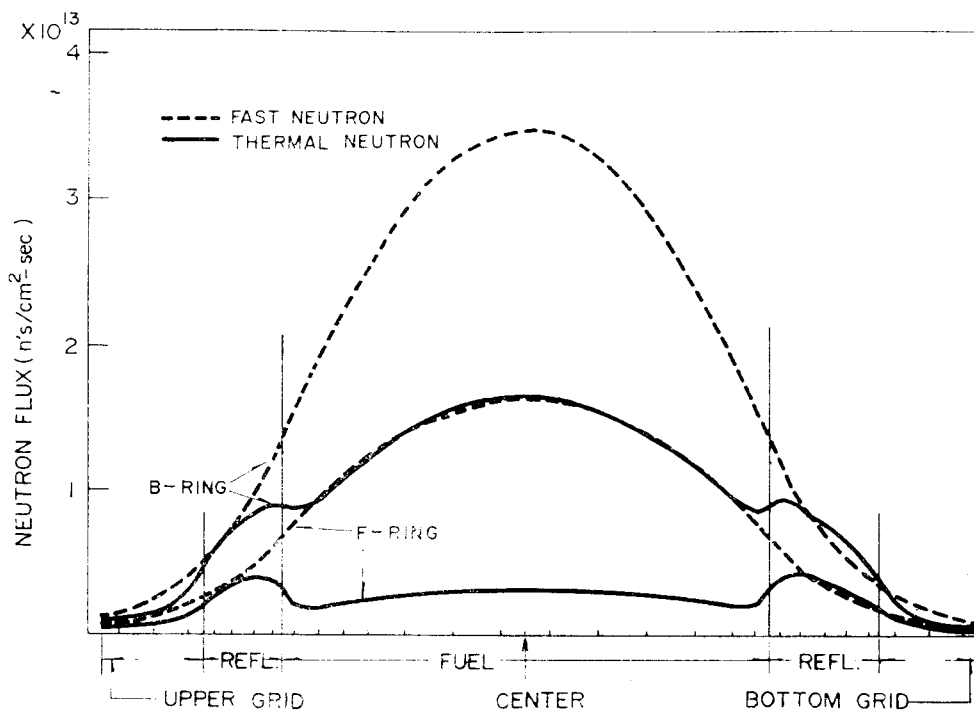


Fig. 11. Fast and Thermal Neutron Flux Distribution in Axial Direction (z) at 1MW

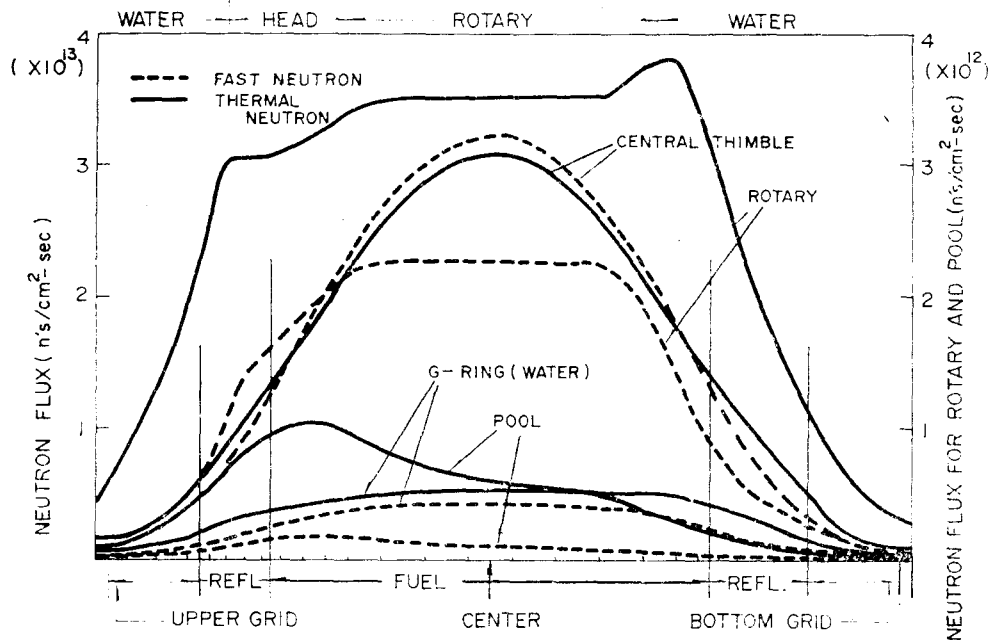


Fig. 12. Fast and Thermal Neutron Flux Distribution in Axial Direction (II) at 1MW

and values between the results of hexagonal and cylindrical calculation are derived from different methods in representation. That is to say that hexagonal geometry fluxes are axially averaged for certain cell while those from cylindrical geometry are ring-averaged for center position of axial direction. Ring-averaged axial flux shapes for the fueled zones are presented in Figure 11, while those for the irradiation facilities are described in Figure 12. Thermal neutron reflection effect in fueled zones is distinguished. Axially flat flux due to void in rotary specimen rack reaches up to 25cm. Flux shape in G-ring water zone is shifted to the bottom direction while that in pool zone which is positioned just outer of rotary specimen rack is shifted to the upper direction. These phenomena are also due to the few interactions of neutron in rotary

specimen rack.

#### 4. Axial Bucklings ( $B_z^2$ )

Accurate determination of axial Bucklings is one of the major tasks to improve reliability of X-Y 2-dimensional calculation especially in case of a small core. An effort was made to generate group and zone dependent bucklings rather than conventional group and/or zone independent ones, since information on space and energy dependent neutron spectrum is more important than power distribution in research reactor. If group and/or zone independent bucklings be used in research reactor analysis some errors might be introduced in neutron spectrum calculation though accurate reactivity and power distribution information can be obtained.

It is verified in this study that axial leakage term to the gross neutron balance

**Table 3. Calculated Buckling Values** ( $\times 10^{-3}$ )

Position Group	Central Thimble	B-ring		FLIP			Rotary	Pool
		Calculated Value	GA	Calculated Value		GA		
				D-ring	F-ring			
1	3.885	4.605	4.1	5.094	5.190	5.55	2.925	3.255
2	3.518	3.267	4.1	4.175	4.084	4.56	2.944	3.308
3	3.094	3.030	4.1	3.123	2.863	3.60	2.370	3.278
4	2.965	2.343	4.1	0.346	-0.180	-0.22	2.143	3.257
5	2.941	3.434	4.1	-0.296	-1.251	6.17	2.212	2.959
6	2.632	-0.920	4.1	-15.94	-18.09	-19.05	2.225	2.748
7	2.534	-6.092	4.1	-41.22	-46.42	-82.7	2.748	2.748

**Table 4. Thermal Neutron Flux, Neutron Temperature and Effective Thermal Cross-Section in Irradiation Facilities (Clean Core, 1.2MW)**

Group Energy (eV)	Thermal Neutron Flux ( $\times 10^{12}$ n's/cm <sup>2</sup> -sec)				Neutron Temperature of Maxwell Distribution (°K)	Effective Neutron Cross Section of Au-foil at 0-0.42eV (barns)
	4	5	6	7		
Position	1.125-0.42	0.42-0.14	0.14-0.05	0.05-0.002		
Central Thimble	1.34	4.22	15.32	17.76	338	78.67
G-3	0.267	0.752	2.61	3.00	340	78.50
G-6(Pneumat.)	0.213	0.614	2.15	2.47	340	78.50
G-17	0.330	0.771	2.49	2.82	342	77.99
G-22	0.390	0.774	2.29	2.57	345	77.32
G-1(water)	0.157	0.689	2.71	3.18	336	79.43
Rotary	0.075	0.294	1.12	1.27	342	78.62
Pool	0.025	0.124	0.496	0.585	335	79.98

\*The Cross-Section for Au is 98.8 barns at 0.0253eV

for TRIGA Mark-III reaches up to 15% and that  $B_1^2$  variation being dependent upon group and zone is quite sensitive.

Bucklings used herein are presented in Table 3 and compared with those from GA. GA's data may be those for the unique core that is loaded with either all FLIP's or all standard fuels. In such sense, they are group-and/or zone-independent.

### II. 5. Thermal Spectra in Irradiation Facilities

Effective thermal neutron temperatures and effective capture cross-sections of gold foil in irradiation facilities, which are derived from the method explained in Section II.5., are presented in Table 4. Each

thermal neutron flux in this table is averaged with respect to volume of each zone.

In case of activation analysis for the measurement of thermal neutron flux, spectrum weighted effective thermal cross-section of the sample should be pre-determined. Neutron spectra can be measured by experiment; however, this requires a great deal of time and efforts because of frequent changes in core conditions. On the contrary, calculational approach can be made use of convenience only if its accuracy is once verified. Spectra calculated in this study are not verified yet due to the lack of experimental data. Yet it can be affirmed that the utilization of the result of

this study will eventually prove to be more reasonable than the previous methods, such as replacement of neutron temperature by coolant temperature.

#### Acknowledgement

The authors wish to express sincere thanks to Messrs. Keon Jung Yoo and Young Jin Kim for their helpful discussion. The authors are also very grateful to the members of the reactor operation group, KAERI, for their assistance.

#### References

1. J.C. Ringle, K. Hornik, A.H. Robinson, "Safety Analysis Calculations for a Mixed and FLIP core in TRIGA Mark-III", TOC-7, TRIGA Owners' Conf. IV, March (1976).
2. Jung Do Kim, Jong Tai Lee and Chong Chul Yook, "Analysis of Standard and FLIP Fuel Mixed Loading Patterns in TRIGA Mark-III Reactor", *J. of the Korean Nuclear Society*, **11**(4), 287 (1979).
3. T.B. Fowler, D.R. Vondy and G.W. Cunningham. "CITATION", ORNL-TM-2496, Rev. 2 (1975).
4. A. J. Gietzen, Private Communication with GAC (1980).
5. Gulf Energy and Environmental System Co., "TRIGA Mark-III Reactor Mechanical Operating and Maintenance Manual", E-117-160 (1972).
6. Gulf General Atomic Inc., "Safeguards Analysis Report for the Korea Atomic Energy Research Institute", GA-9867 (1970).
7. Jong Tai Lee, Jung Do Kim and Mann Cho, "Multigroup Calculations for TRIGA-Type Reactor Analysis", *J. of the Korean Nuclear Society*, **10**(2), 87 (1978).
8. Bell and Glasstone, "Nuclear Reactor Theory", Van Norstrand Reinhold (1970).
9. John R. Lamarsh, "Introduction to Nuclear Reactor Theory", Addison-Wesley Co. (1966).
10. James J. Duderstadt and Louis J. Hamilton, "Nuclear Reactor Analysis", Wiley (1976).
11. A. Shmizu, "Calculation of the Effective Thermal Cross Section and Its Temperature Coefficient-I", *J. Atomic Energy Soc. (Japan)*, **2**(10) 611-617 (1960).
12. C.H. Westcott, "Effective Cross-Section Values for Well-Moderated Thermal Reactor Spectra", CRRP-960 (1960).